Hindawi

Research Article

Influencing Factors of Interfacial Behavior between Geogrid and Coal Gangue

Xiangxi Fan,[1,2] Pengfei Gao,[3,4] Weichao Liu [3,4] Lingxiao Meng,[2,5] Yingdong Xu,[2,5] and Hong Zheng[6]

[1]*China University of Mining and Technology (Beijing), Beijing 100083, China*
[2]*China State Construction Engineering Corporation Limited, Beijing 100029, China*
[3]*State Key Laboratory of Mechanical Behavior and System Safety of Traffic Engineering Structures,*
 Shijiazhuang Tiedao University, Shijiazhuang 050043, China
[4]*School of Civil Engineering, Shijiazhuang Tiedao University, Shijiazhuang 050043, China*
[5]*China Construction Infrastructure Corporation Limited, Beijing 100000, China*
[6]*BOSTD Geosynthetics Qingdao Ltd., Qingdao 266000, China*

Correspondence should be addressed to Weichao Liu; liuweichao@stdu.edu.cn

Coal gangue is a type of solid waste that is generated in the process of coal mining and washing. This concept can be effectively used in reinforced engineering fillings. The influences of shear rates and geogrid transverse ribs were studied using a large indoor direct shear test. The test results showed that the relationship between shear stress and shear displacement of geogrid-coal gangue is nonlinear, and the shear process is accompanied by the crushing of coal gangue particles. The addition of geogrid significantly improved the shear stress and interfacial quasi-cohesion of geogrid-coal gangue, whereas the interfacial quasi-friction angle remained almost unaffected. When normal stress was greater than 25 kPa, the shear stress gradually increased as the shear rate was increased from 1 to 5 mm/s. With an increasing shear rate, the interfacial quasi-friction angle increased, whereas the interfacial quasi-cohesion decreased. The interfacial shear stress, interfacial adhesion, and interfacial friction angle decreased with the number of geogrid ribs; the contribution of the middle transverse rib to the interfacial shear strength was smaller than that of the transverse rib at the far end in the shearing direction.

1. Introduction

Coal gangue is a type of solid waste with low carbon content and is produced in the process of coal mining and washing. Large quantities of coal gangue stacked in the open spaces occupy a significant amount of land, pollute air, soil, and water resources. Furthermore, they can cause landslides, which seriously affect the surrounding ecological environment and personal safety of residents. Therefore, harm-prevention and utilization methods for coal gangue are of great significance. Using coal gangue as a filling in subgrades [1] and reinforced-soil retaining walls [2] not only helps recycle the waste but also reduces the occupation of land due to coal gangue storage and provides significant economic and social benefits.

When coal gangue is used as a filler in reinforced structural engineering, the interfacial parameters between the coal gangue and reinforced material are important and can be measured using pull and shear tests. Using the direct shear test, Yang and Sui [3] noted that the interfacial friction angle and quasi-cohesion between clay and geogrid increased with an increase in the shear rate. Zhang et al. [4] found that an increase in the shear rate increased the shear stiffness of the interface between geogrid and clay. By using cyclic shear tests on geogrid and sand, Liu et al. [5] found that the shear characteristics of sand changed from shear softening to shear hardening with an increase in the cyclic shear rate. In addition, Xiao et al. [6] reported that the shear stress at the interface between a three-dimensional geogrid

and sand gradually decreased with an increase in the shear rate. Jin et al. [7] studied the influence of transverse rib spacing of the geogrid on the characteristics of soil-interface reinforcement using pull-out tests, and the results showed that with an increase in the transverse rib spacing, the maximum pull-out force of the geogrid gradually decreased, and the interfacial cohesion and friction angle also showed a decreasing trend. Xiao et al. [8] analyzed the effects of interfacial normal stress, transverse rib percentage, grid width, and pulling rate on the interfacial characteristics between biaxial geogrid and sand using pull-out tests. Xu et al. [9] analyzed the influence of upper cover pressure, water content, geogrid size, and pulling rate on the friction coefficient of the interface between geogrid and expansion soil.

Teixeira et al. [10] found that there was an optimal geogrid transverse rib spacing according to the results of a pull-out test, and when the spacing was smaller than this value, the two adjacent transverse ribs had a mutual effect and reduced the pull-out force. Palmeira [11] reported that the friction resistance between the grid and sand surface accounted for a larger proportion of the pulling force when the pulling displacement was small and that the passive resistance of the sand to the geogrid accounted for a larger proportion of the pulling force when the pulling displacement was large. Tavakoli Mehrjardi et al. [12] noted that a geocell with an aspect ratio of four performed the best in improving the interfacial shear strength through direct shear tests and suggested that the geocell should be used under conditions of coarse particles and low normal stress. Ling et al. [13] compared the interfacial friction characteristics between an original geogrid and a geogrid with the transverse ribs removed and found that the transverse ribs of the geogrid had a significant influence on the interfacial characteristics of the reinforcement and soil, with a contribution rate of more than 50%. Alagiyawanna et al. [14] changed the numbers of longitudinal and transverse ribs of a geogrid in pull-out tests to study the contribution and effect of the longitudinal and transverse ribs on the pull-out force, respectively.

There are many studies on the interfacial characteristics between reinforcement materials and soil or sand, but only few on the reinforcement mechanism between coal gangue and geosynthetics. In this study, large-scale direct shear tests on burned coal gauge and uniaxial geogrid are conducted under different normal stresses, shear rates, and transverse rib numbers to analyze their impact on the interfacial characteristics of burned coal gangue and geogrid. The results of this study can provide reference for better application of coal gangue to reinforcement structures.

2. Materials and Methods

2.1. Materials.
The reinforcement material selected in this test is the uniaxial tensile high density polyethylene (HDPE) geogrid. According to the size of the test box, the geogrid width (B) is 1 m, as shown in Figure 1. The technical indicators are listed in Table 1.

The coal gangue was obtained from the LuBi construction material field in Laiwu, Shandong Province, China, which has been stored for approximately 40–50 years and has a stacking volume of 1.07 million m^3. The physical and mechanical indices of the gangue were obtained using gradation and direct shear tests, and they have been listed in Table 2; the grading curve of the particles is shown in Figure 2.

2.2. Test Method.
Presently, Yang and Sui [3], Li et al. [15], Xu and Shi [16], Fleming et al. [17], and other scholars locally and abroad have adopted the direct shear test to study the characteristics of the reinforcement soil interface between geosynthetics and fillers and have achieved good research results. Therefore, considering the limitations of test equipment, the direct shear test was used in this study.

2.3. Test Apparatus.
The test instrument is a large pull-out and direct shear apparatus. The test equipment set consists of four parts: loading device, traction device, test box, and data acquisition system.

The test box is divided into upper and lower parts, and the internal dimensions of the upper part are $1000 \times 1000 \times 370$ mm (length × width × height), while the dimensions of the lower part are $1300 \times 1000 \times 370$ mm. The normal stress is induced by the pneumatic reaction system with a maximum pressure of 400 kPa. The horizontal tension is induced by the motor system, and the shear rate range is 0–5 mm/min. The front and rear ends of the test box are each equipped with high-precision displacement sensors. The shear test data are automatically collected by the software system that is matched with the load and displacement sensors.

The direct shear apparatus used in this study is shown in Figure 3. Figures 3(a) and 1–11 denote the displacement meter, geogrid fixture, geogrid, traction motor, lower shear box filler, upper shear box filler, upper shear box, lower shear box, rigid pressure plate, flexible air pressure bag, and cover plate of the reaction force, respectively. During the test, the lower shear box was fixed and the upper shear box was pushed to the right to apply the shear force to the geogrid and coal gangue.

2.4. Test Scheme.
The purpose of this study was to investigate the influence of transverse rib percentage and shear rate on the interfacial characteristics of the geogrid and burned gangue. Thus, three different percentages of transverse ribs and three shear rates were chosen. The length of the geogrid sample was 1 m, and special scissors were used to trim the geogrid transverse ribs. The number of transverse ribs accounted for 100, 75, and 50% of the transverse ribs in the original sample, respectively. The three shear rates were 1, 3, and 5 mm/min, and normal stresses of 25, 50, 100, and 150 kPa were selected. As shown in Figures 4–6, the serial number of geogrid ribs located inside the shear box from left to right is 1, 2, 3, and 4, respectively. The geogrid with 75% of the original transverse rib number was the case for which the third transverse rib was cut off, and the grid with 50% of the original transverse rib number was the case for which the third and fourth transverse ribs were cut off.
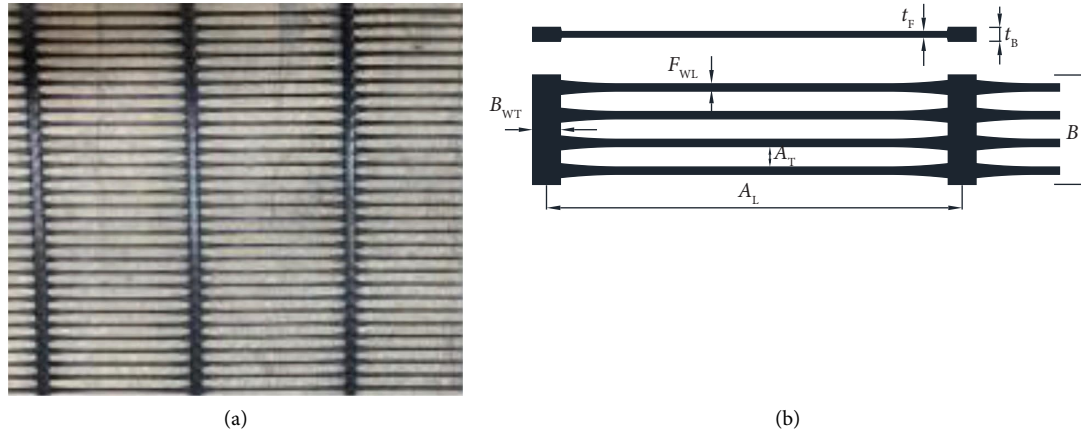
(a)   (b)

FIGURE 1: Uniaxial HDPE geogrid. (a) Object image. (b) Schematic.

TABLE 1: Technical indicators of the geogrid.

Center spacing of the transverse rib (A_L) (mm)	Ultimate tensile strength (F_u) (kN/m)	2% strain strength ($F_{2\%}$) (kN/m)	5% strain strength ($F_{5\%}$) (kN/m)	Peak strain (ε_P) (%)
263.8	97.3	27.2	52.8	11.6
Thickness of the transverse rib (t_B) (mm)	Width of the transverse rib (B_{WT}) (mm)	Thickness of the longitudinal rib (t_F) (mm)	Width of the longitudinal rib (F_{WL}) (mm)	Grid spacing between the longitudinal ribs (A_T) (mm)
3.93	18.42	1.23	5.28	16.80

TABLE 2: Mechanical indices of the coal gangue.

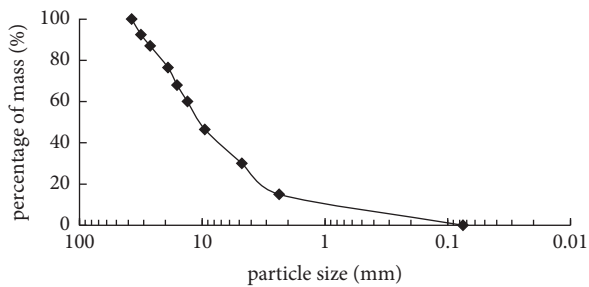| Maximum dry density (ρ_{dmax}), g/cm³	Apparent density (ρ_a), g/cm³	Apparent dry density (ρ_{ad}), g/cm³	Bulk density (ρ_b), g/cm³	Uniformity coefficient (C_u)	Curvature coefficient (C_c)	Cohesion (c), kPa	Angle of friction (φ)°
2.03	2.665	2.372	2.197	14.35	1.85	0.84	32.21

FIGURE 2: Gradation curve of gangue particles.

Owing to the large size of the test box, to reduce the installation and disassembly time, the experimental scheme was set up according to reference [18], and the lower chamber was placed without removing the rigid material, and geogrids and fillers were laid over the rigid materials.

This test scheme can be used to simulate the working conditions of geogrid reinforcement at the back of the abutment and the characteristics at the interface between new and old subgrades in subgrade-widening projects. The stiffness of an old subgrade is much greater after service for a period of time than that of a new subgrade, and differential settlement can easily occur at the interface between the new and old subgrades because of the differences in their stiffness. In engineering, geogrids are often laid at the interface between new and old subgrades to reduce differential settlement. Furthermore, it could also provide a reference for future research on interfacial characteristics of different fillers above and below the geogrid.

The specific test cases are shown in Table 3.

The compaction degree of the coal gangue in the test was 93%, and the total height was 25 cm. The filler was compacted using an electric impact ram in three layers, and the heights of each layer were 8, 8, and 9 cm, respectively. The specific test steps are as follows: (1) Start the equipment, and check whether the components are running normally. (2) Load the rigid material into the lower shear box. (3) Cut, lay, and fix the geogrids. (4) Apply Vaseline evenly to the inner wall of the upper shear box, fill coal gangue of corresponding quality, and compact it. After compaction, shave the surface, and repeat this step to fill the second and third layers of coal
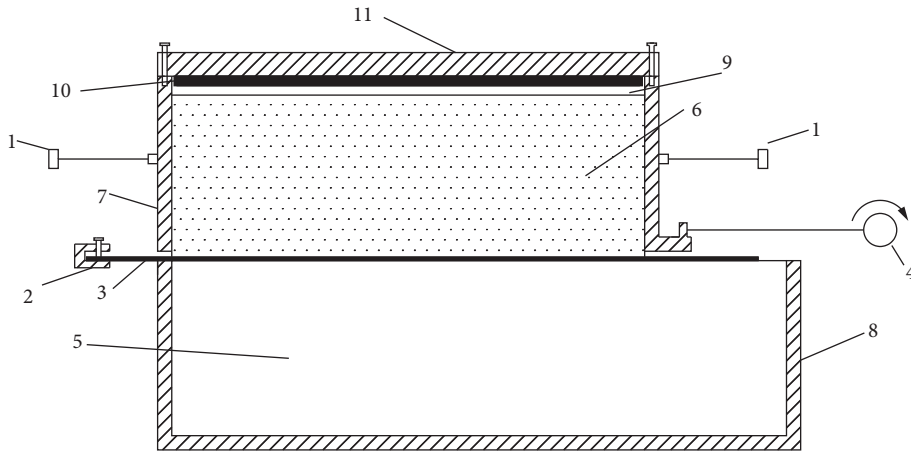
(a)

(b)

FIGURE 3: Direct shear apparatus. (a) Sectional view of shear boxes. (b) Object picture.
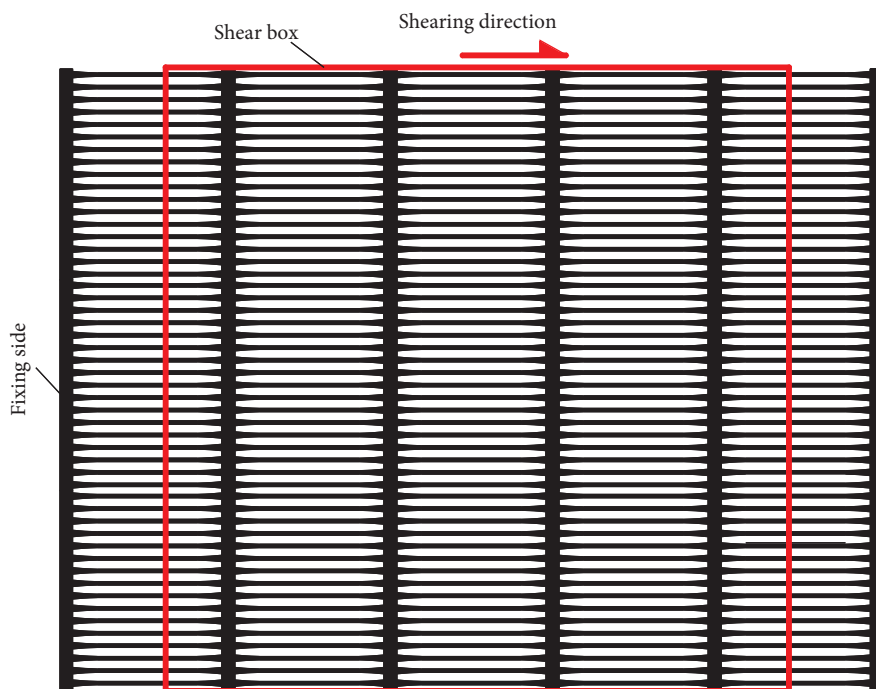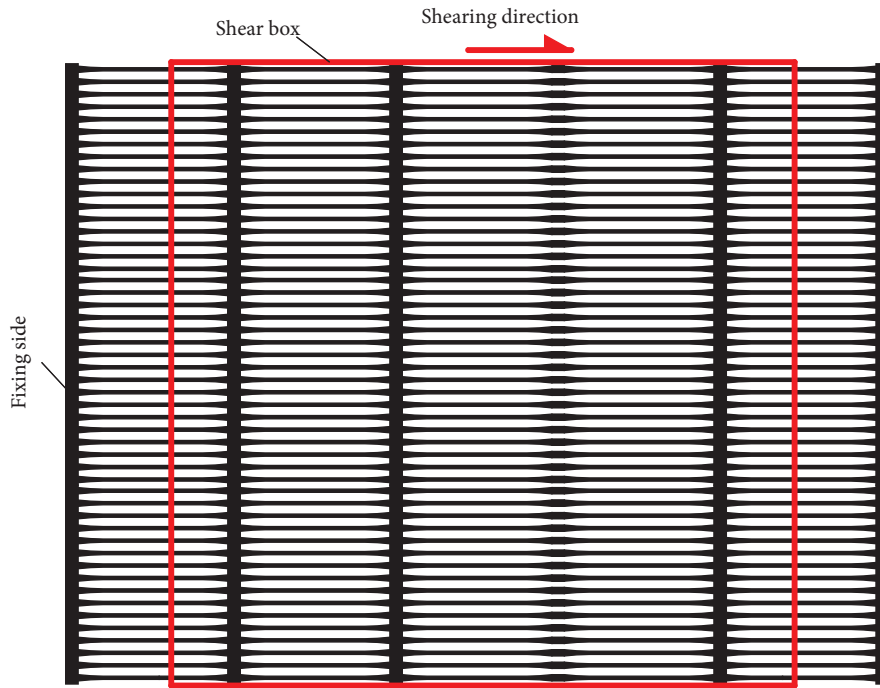

FIGURE 4: Geogrid with 100% cross ribs.
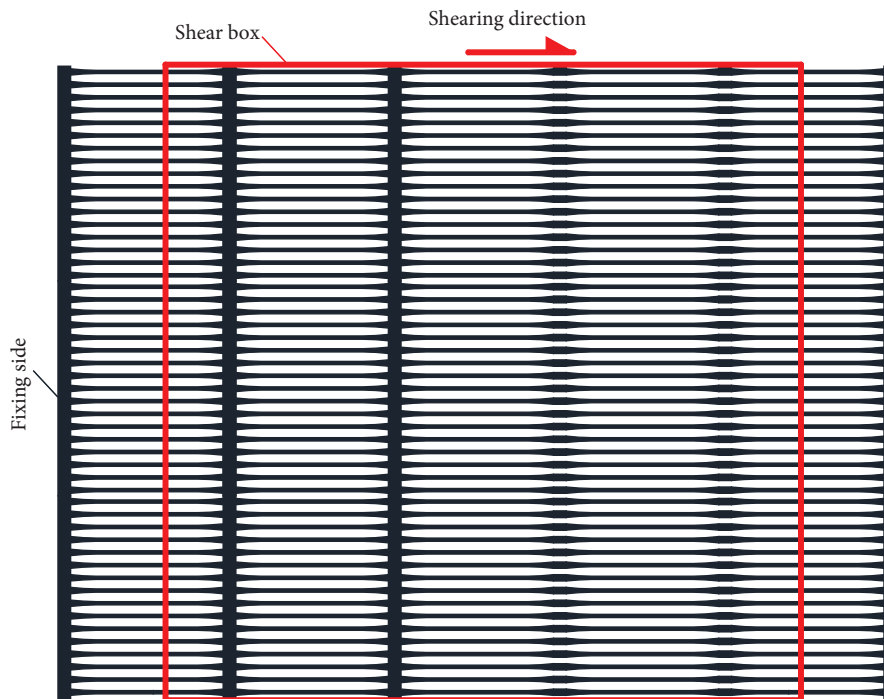
FIGURE 5: Geogrid with 75% cross ribs.

FIGURE 6: Geogrid with 50% cross ribs.

gangue. (5) Lay a rigid pressure plate on the upper coal gangue surface, confirm uniformity and no shaking, lay flexible air pressure bag, and connect compressed air. (6) Fix the cover plate of the reaction force, apply the normal load, and read the normal load through the pressure gauge. Maintain the normal load for 10 min, set the shear rate according to the test scheme, and perform the shear. (7) After completing the initial set of steps, restore the instrument to the initial state, and repeat steps (3) to (6) to conduct the next set of experiment steps.
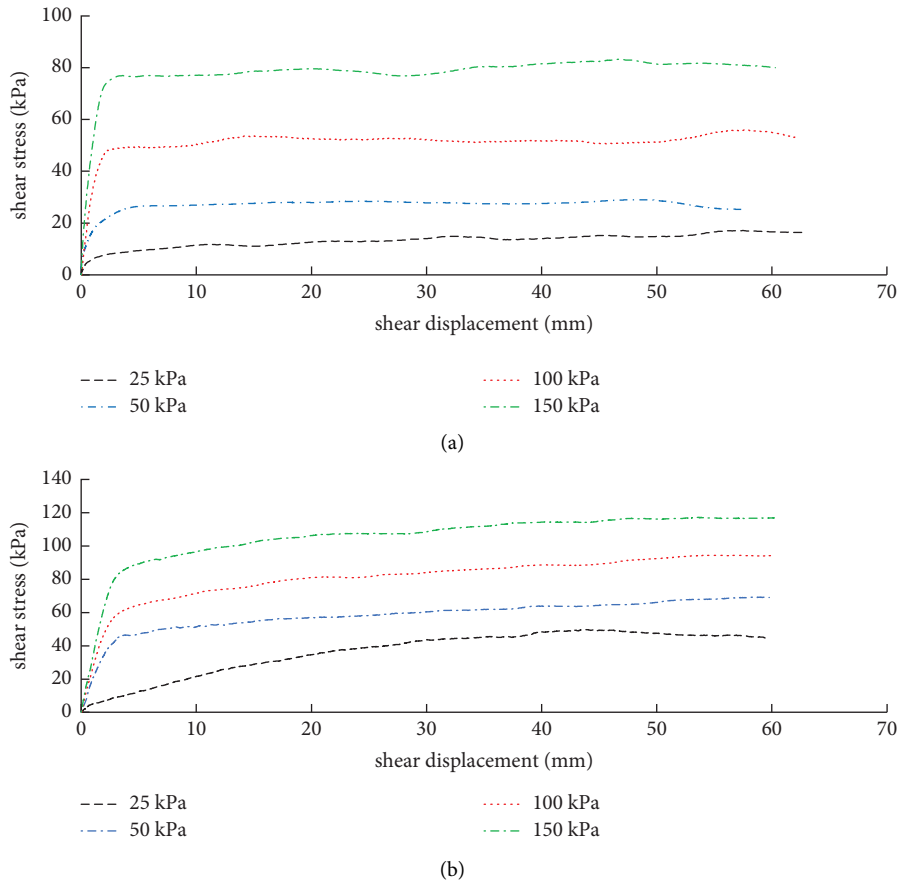
(a)

(b)

FIGURE 7: Curve of relationship between shear stress and shear displacement. (a) Case 1: gangue without geogrid. (b) Case 2: gangue with geogrid.
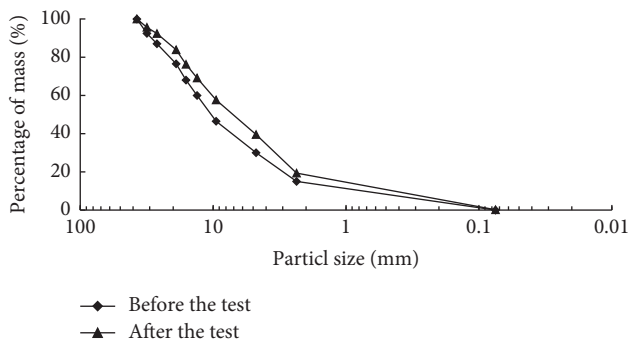

FIGURE 8: Coal gangue particle gradation curve before and after the test.
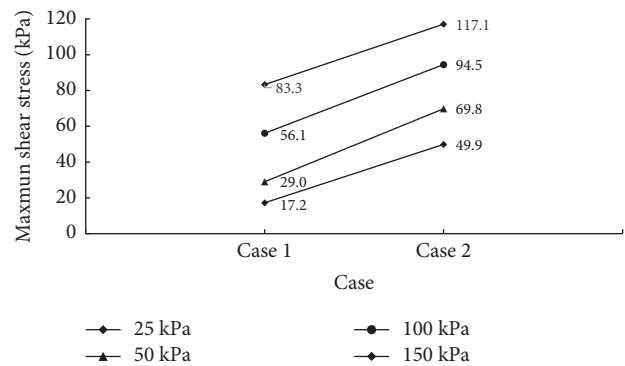

FIGURE 9: Variation of the maximum shear stress.

3. Results

3.1. Change in Interface Characteristics of Coal Gangue due to Grid. According to the test data of Cases 1 and 2 under different normal stresses, the plots of the relationship between shear stress and shear displacement were obtained, as shown in Figure 7.

From Figure 7, it can be observed that the relationship between shear stress and shear displacement is nonlinear and can be mainly divided into two stages; in the first stage,

the shear stress rapidly increases with increasing shear displacement, and in the second stage, the shear stress gradually stabilizes or slowly increases with increasing shear displacement.

When the normal stress is small ($\sigma_v = 25$ kPa), the shear stress gradually and linearly increases with the shear displacement and then decreases after reaching a peak value, as can be observed from Figure 7(b). It can be seen that a large shear displacement is needed so that the shear force between the coal gangue particles and the geogrid can increase slowly.
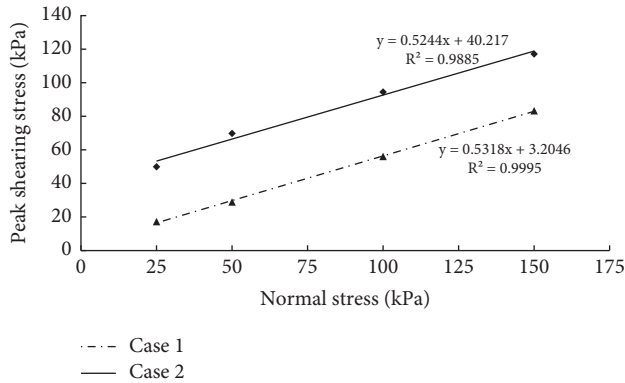
FIGURE 10: Fitting curve of shear strength.

FIGURE 11: Variation curve of shear strength parameters.

When the normal stress is large ($\sigma_v > 25$ kPa), the curve rapidly reaches the second stage, which is accompanied by a shear hardening tendency. In addition, the strain hardening phenomenon is due to the gangue deforming by shear shrinkage under the action of high normal stress; the shear process is accompanied by the fragmentation of the coal gangue particles. The particle gradation curves of the coal gangue before and after the test are shown in Figure 8.

The fine particles increased and filled the gaps between the large particles of the coal gangue, making the coal gangue denser with the increase in the shear displacement and gradually increased its occlusion with the mesh and transverse ribs of the geogrid.

The maximum shear stress variation under different normal stresses in Cases 1 and 2 is shown in Figure 9.

The maximum shear stress increases from 17.2 to 49.9 kPa, 29.0 to 69.8 kPa, 56.1 to 94.5 kPa, and 83.3 to 117.1 kPa when the normal loads are 25, 50, 100, and 150 kPa, respectively; the increments are 32.7, 40.8, 38.4, and 33.8 kPa; and the increase rates are 190.12, 140.69, 68.45, and 40.58%, respectively. It can be seen from Figure 9 that the interfacial shear stress significantly increases with the addition of geogrid, but the increased proportion decreases with the increase of the normal stress.

The shear strength indices of the reinforcement soil interface include the friction angle and quasi-cohesion. The shear strength curves of the interface between the geogrid and coal gangue in cases 1 and 2 are plotted (Figure 10) from the normal and peak shear stresses, and the variations in the interfacial shear strength parameters are shown in Figure 11.

It can be seen from Figure 11 that after the geogrid is added, the interfacial friction angle changes from 28.00 to 27.67°, with little decrease of 1.14%; the interfacial quasi-cohesion significantly increases from 3.20 to 40.22 kPa, with an increase of 1156.88%, so the interfacial shear strength significantly increases after the geogrid was added; this was mainly reflected by the increase in interfacial quasi-cohesion. The reason is possibly that coal gangue particles can be well combined and interlocked with geogrid mesh and transverse rib, and a certain thickness of the shear band is generated near the shear plane.
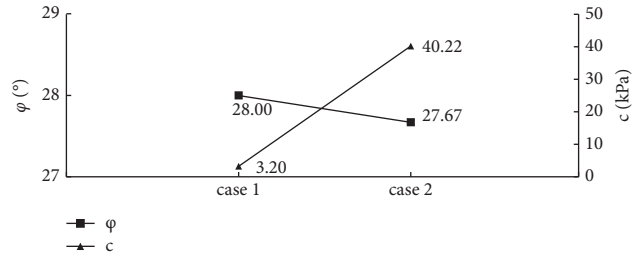
3.2. Effect of Shear Rates. The relationship curve of shear stress and shear displacement was obtained according to the test data of three different shear rates under different normal stresses, as shown in Figure 12. It can be observed that the shear rate does not change the trend of the curve of the shear stress and shear displacement. The curve could still be divided into a linear-increase stage and stable- or gradual-increase stage. As can be observed from Figure 12(c), when the shear rate is 5 mm/min, the normal load is 150 kPa and the shear displacement reaches 47 mm; the applied stress exceeds the ultimate strength of the longitudinal ribs of the geogrid, which results in the failure of some longitudinal ribs and a decrease in the shear stress.

The maximum shear stress variation diagram under the three shear rates and different normal stresses were obtained, as shown in Figure 13. When the normal stress is 25 kPa, the changes in the shear rate have little effect on the maximum shear stress at the interface. When the normal stress is greater than 25 kPa, the interfacial shear stress increases with the shear rate. From Tables 1–3, when the normal stress is 50, 100, and 150 kPa and the shear rate increased from 1 to 5 mm/min, the maximum shear stress increment is 32.2 kPa, which indicates an increase by 27.58%. Furthermore, the greater the normal stress, the greater the increase in the shear stress.

Figures 14 shows the shear strength curves of the interface between the geogrid and coal gangue reinforcement soil under three shear rates, while Figure 15 shows the change in the interfacial shear strength parameters.

With an increasing shear rate, the interfacial friction shows an increasing trend (Figure 15), and its value increases from 27.67° at 1 mm/min to 37.94° at 5 mm/min, which is an increase by 37.12%. This is because during the shear process, the coal gangue particles near the shear plane may roll and rearrange, which may decrease the bite force between the particles and require a certain amount of time to complete. When the shear rate is large, the time of the direct shear process of the coal gangue is not sufficient for the particles to complete the rearrangement, which increases the bite effect of the coal gangue particles and increases the interface friction angle. The interfacial quasi-cohesion decreases from 40.22 kPa at 1 mm/min to 35.95 kPa at 5 mm/min, which is a decrease of 10.62%, and with an increase in the shear rate, the quasi-cohesion between the coal gangue and geogrid does not come into full effect when the shear rate is large.

It can be seen that when the shear rate is small, the quasi-cohesion at the interface between the geogrid and coal gangue easily comes into effect, whereas when the shear rate
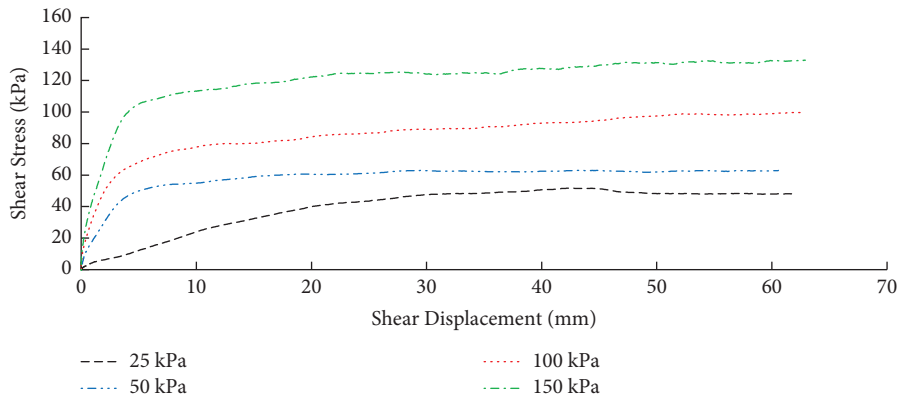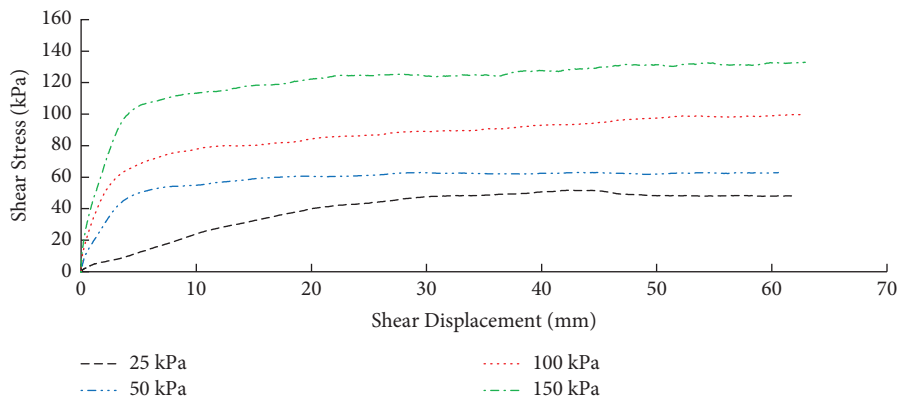
TABLE 3: Test cases.

Cases	Geogrid condition	Shear rate (mm/min)	Normal stress (kPa)	Maximum shear displacement (mm)
Case 1	No grid	1		
Case 2	100% transverse ribs	1	25	
Case 3	100% transverse ribs	3	50	
Case 4	100 %transverse ribs	5	100	60
Case 5	75% transverse ribs	5	150	
Case 6	50% transverse ribs	5		
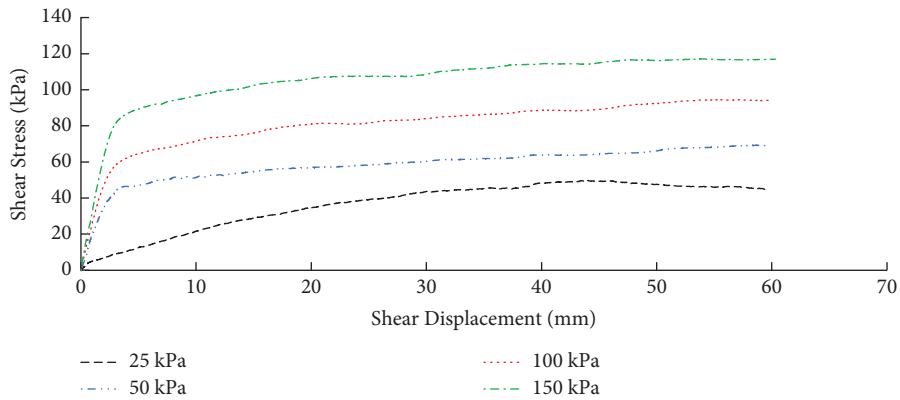
(a)

(b)

(c)

FIGURE 12: Relationship curve between shear stress and shear displacement under different shear rates. (a) Shear rate of 1 mm/min. (b) Shear rate of 3 mm/min. (c) Shear rate of 5 mm/min.
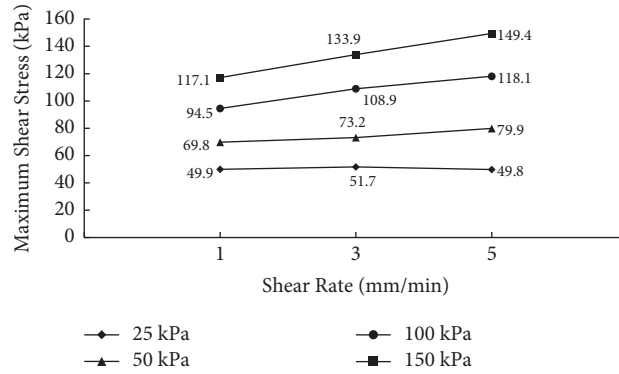
FIGURE 13: Variation curve of the maximum shear stress under different shear rates.

TABLE 4: Change in shear stress with shear rate.

Normal stress (kPa)	Shear rate (mm/min)	Maximum shear stress (kPa)	Shear stress increment due to shear rate change (kPa)			Increase in shear stress due to change in shear rate (%)		
			1–3	1–5	3–5	1–3	1–5	3–5
50	1	69.8	3.4	10.1	6.7	4.87	14.47	9.15
	3	73.2						
	5	79.9						
100	1	94.5	14.4	23.6	9.2	15.24	24.97	8.45
	3	108.9						
	5	118.1						
150	1	117.1	16.8	32.3	15.5	14.35	27.58	11.58
	3	133.9						
	5	149.4						

Note. 1–3 in Table 4 indicates that the shear rate changed from 1 to 3 mm/min.

FIGURE 14: Fitting curve of shear strength under different shear rates.
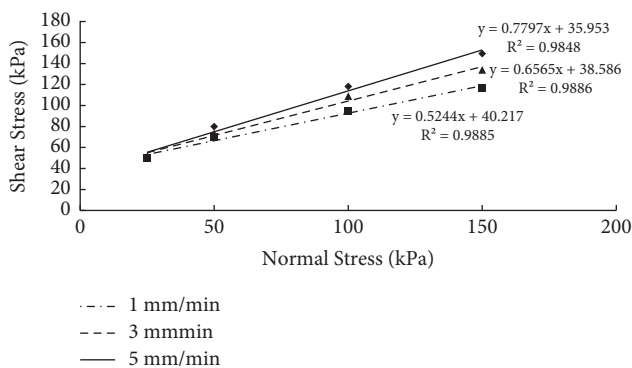

FIGURE 15: Variation curve of the interfacial shear strength parameters under different shear rates.

is large, the bite friction between particles plays a major role. Different shear rates can be used to study the interface characteristics of engineering structures in different failure stages. Using discrete element simulations, Duan et al. [19] concluded that the failure of a slope can be divided into low-speed creep, high-speed slip, deceleration, and self-stabilizing adjustment stages. The slip speed at each stage of the landslide was different. Furthermore, it was suggested to use
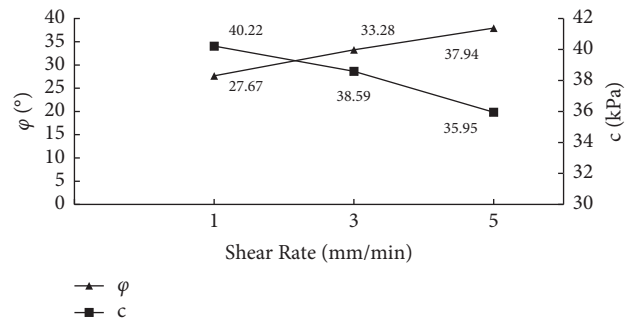
low shear rate to study the low-speed creep stage and to use high shear rate to study the high-speed slip stage for engineering applications.

3.3. Effect of Percentage of Geogrid Transverse Ribs.
According to the test data of three different transverse rib percentages of the geogrid under different normal stresses, the relationship curve between the shear stress and shear displacement was obtained, as shown in Figure 16. The change in
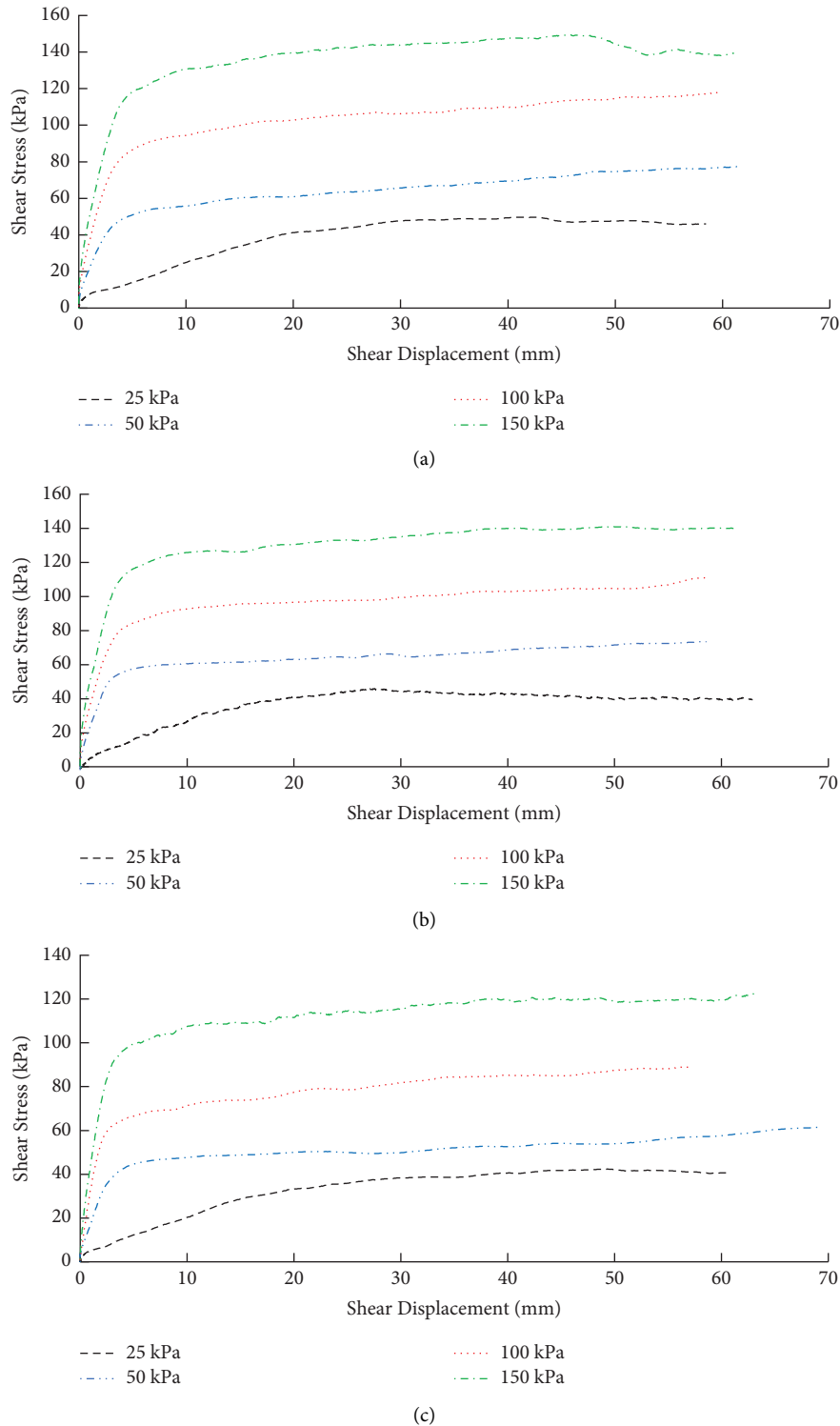
(a)

(b)

(c)

FIGURE 16: Relationship curve between shear stress and shear displacement under different percentages of the transverse ribs of the geogrid. (a) 100% geogrid transverse ribs. (b) 75% geogrid transverse ribs. (c) 50% geogrid transverse ribs.

the number of transverse ribs did not affect the shape of the relationship curve between the shear stress and shear displacement.

Figure 17 shows the maximum shear stress variation diagram under different transverse rib percentages of three geogrids with different normal stresses.

It can be seen from Figure 17 that the interfacial shear stress gradually decreases with the decrease in the percentage of geogrid transverse ribs. When the normal stress is 25 kPa, the shear stress linearly decreased linearly, as the percentage of the geogrid transverse ribs changes from 100 to 50%. When the normal stresses are 50, 100, and 150 kPa, the shear
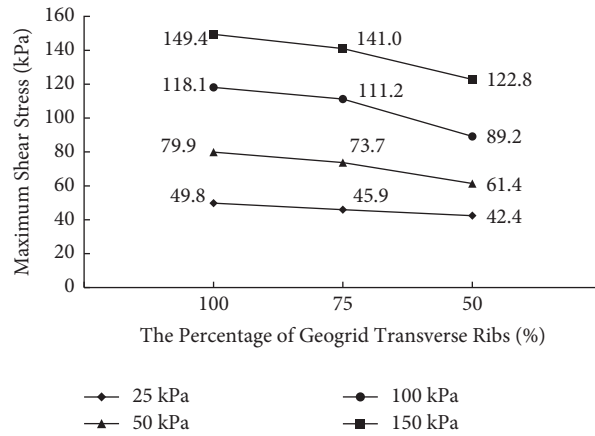
FIGURE 17: Variation curve of the maximum shear stress under different transverse rib percentages of the geogrid.

TABLE 5: Variation of the shear stress caused by different transverse rib percentages of the geogrid.

Normal stress (kPa)	Percentage of geogrid transverse ribs (%)	Maximum shear stress (kPa)	Reduction of shear stress caused by percentage change in the number of geogrid transverse ribs (kPa)			Shear stress reduction caused by the percentage change of geogrid transverse ribs (%)		
			100–75	100–50	75–50	100–75	100–50	75–50
25	100	49.8						
	75	45.9	3.9	7.4	3.5	7.83	14.86	7.63
	50	42.4						
50	100	79.9						
	75	73.7	6.2	18.5	12.3	7.76	23.15	16.69
	50	61.4						
100	100	118.1						
	75	111.0	6.9	28.9	22.0	5.84	24.47	19.78
	50	89.2						
150	100	149.4						
	75	141.0	8.4	26.6	18.2	5.62	17.80	12.91
	50	122.8						

Note. 100-75 in Table 5 indicates that the percentage of geogrid transverse ribs changes from 100% to 75%.

stress nonlinearly reduces, as the percentage of geogrid transverse ribs changes from 100 to 50%. From Table 5, the maximum decrease in shearing stress due to the reduction in the number of transverse ribs of the geogrid is 24.47%; when the normal stress is 50, 100, and 150 kPa, the reduction in shear stress due to the change in the percentage of the geogrid transverse ribs from 100 to 75% is 7.76, 5.84, and 5.62%, respectively while that from 75 to 50% is 16.69, 19.78, and 12.91%, respectively.

The shear strength curve at the interface between the geogrid and coal gangue under different percentages of the geogrid transverse ribs is shown in Figure 18, and the change in the shear strength parameters of the interface is shown in Figure 19.

It can be seen from Figure 19 that with the decrease of the geogrid transverse ribs, the interfacial friction angle and quasi-cohesion show a downward trend; among

them, the decrease in the interfacial quasi-cohesion is approximately linear, so each transverse rib produces roughly the same quasi-cohesion force. When the percentage of the geogrid transverse ribs changes from 100% to 50%, the interfacial quasi-cohesion changes from 35.95 to 27.73 kPa, with a decrease of 22.87%; and the interfacial friction angle decreases from 37.94 to 36.80°, with a decrease of 3.00%. When the percentage of cross ribs of the geogrid changes from 75% to 50%, the interfacial friction angle significantly decreases (i.e., from 36.80 to 32.23°), with a decrease of 12.42%, whereas the decrease in the interfacial friction angle is 15.05% compared to the geogrid with 100% transverse ribs. The transverse rib at the far end in the shearing direction is higher than that of the third rib (in the middle). This may be because the transverse rib at the end could provide greater occlusal friction.
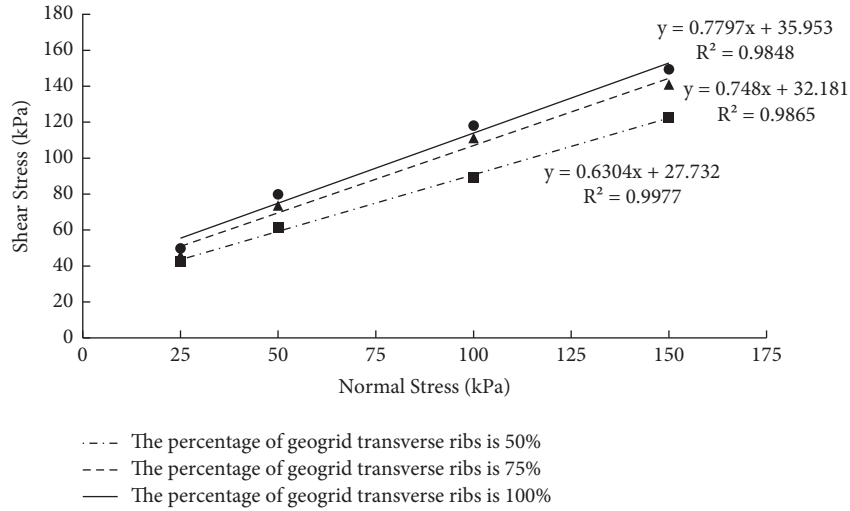
FIGURE 18: Fitting curve of shear strength under different percentages of geogrid transverse ribs.
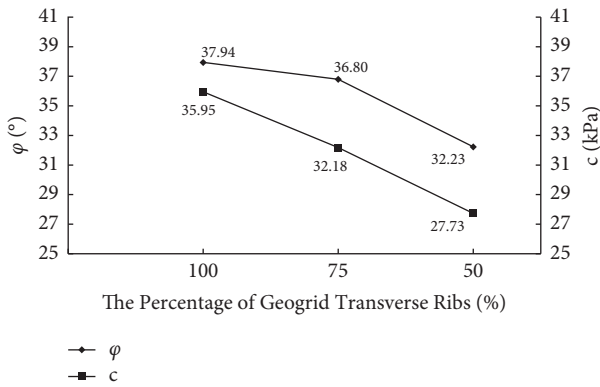

FIGURE 19: Variation curve of interfacial shear strength parameters under different percentages of geogrid transverse ribs.

4. Conclusions

In this study, using a large-scale direct shear test, the influence of shear rate and percentage of the transverse ribs of a geogrid on the interfacial characteristics between geogrid and coal gangue were investigated, and the following conclusions were drawn.

(1) The curve of the relationship between the shear stress and shear displacement of coal gangue reinforced by geogrid obtained from the direct shear test was nonlinear; the shear stress increased with increasing normal stress, and the shear process was accompanied by the crushing of coal gangue particles. The number of fine particles in the coal gangue significantly increased after the test.

(2) Geogrid and coal gangue interacted well in the reinforced structure. Compared with nonreinforced coal gangue, the addition of a geogrid significantly improved the interfacial shear stress and interfacial quasi-cohesion but had little effect on the interfacial friction angle.

(3) The shear rate had a significant effect on the friction characteristics of the interface between geogrid and coal gangue. When the normal stress was greater than 25 kPa, the interfacial shear stress and interfacial friction angle increased with an increase in the shear rate, but the interfacial quasi-cohesion decreased. To study the interfacial characteristics in actual projects, the selection of suitable shear rates is suggested.

(4) With the decrease in the number of transverse ribs, the maximum interfacial shear stress, interfacial friction angle, and interfacial quasi-cohesive force all showed a decreasing trend. The decrease of the interfacial quasi-cohesive force showed a linear trend, and the interfacial friction angle nonlinearly decreased. The transverse rib at the far end provided greater occlusal friction, while the adhesive forces produced by the transverse ribs had approximately equal magnitudes. Therefore, more attention should be paid to protecting the geogrid ribs at the ends in construction.

Data Availability

The data used to support the findings of this study are included within the article.

Conflicts of Interest

The authors declare that they have no conflicts of interest.

Acknowledgments

References

[1] J. Wu, W. H. Gao, Z. T. Zhang, X. Y. Tang, and M. H. Yi, "Study on strength and deformation characteristics of coal

gangue subgrade filling," *Journal of Railway Science and Engineering*, vol. 18, no. 4, pp. 885–891, 2021.

[2] G. L. Yang, Z. Z. Zhang, Y. L. Du, and Y. L. Lin, "Study of coal gangue composite reinforced retaining wall embankment slope by using site tests," *Journal of Railway Science and Engineering*, vol. 14, no. 7, pp. 1382–1390, 2017.

[3] G. Q. Yang and C. Y. Sui, *Journal of Shijiazhuang Railway Institute (Natural Science)*, vol. 23, no. 2, pp. 46–52, 2010.

[4] J. F. Zhang, X. Q. Wang, W. L. Zou, and J. H. Wen, "Experimental study on shear strength parameters and shear stiffness behavior of soil-geogrid interface," *Journal of Yangtze River Scientific Research Institute*, vol. 31, no. 3, pp. 77–83, 2014.

[5] F. Y. Liu, P. Wang, J. Wang, and Y. Q. Cai, "Cyclic and post-cyclic shear behavior of sand-geogrid interface under different shear rates," *Chinese Journal of Rock Mechanics and Engineering*, vol. 35, no. 2, pp. 387–395, 2016.

[6] H. L. Xiao, L. Yu, and L. H. Li, "Analysis of interface friction characteristics of geo-synthetics and sand," *Yangtze River*, vol. 43, no. 7, pp. 56–58+80, 2016.

[7] J. Jin, G. Q. Yang, and W. C. Liu, "Experimental study on effect of transverse rib spacing on geogrid pull-out characteristics," *China Railway Science*, vol. 38, no. 5, pp. 1–8, 2017.

[8] C. Z. Xiao, Y. N. Luo, Z. H. Wang, and H. L. Hu, "Pull-out test of interface characteristics between geogrid and sand," *Journal of Shenzhen University Science and Engineering*, vol. 36, no. 3, pp. 252–259, 2019.

[9] L. R. Xu, J. M. Ling, B. C. Liu, and L. Baochen, "Experimental on interface friction coefficient parameters between geogrids and expansive soil," *Journal of Tongji University*, vol. 32, no. 2, pp. 172–176, 2004.

[10] S. H. C. Teixeira, B. S. Bueno, and J. G. Zornberg, "Pullout resistance of individual longitudinal and transverse geogrid ribs," *Journal of Geotechnical and Geoenvironmental Engineering*, vol. 133, no. 1, pp. 37–50, 2007.

[11] E. M. Palmeira, "Soil–geosynthetic interaction: modelling and analysis," *Geotextiles and Geomembranes*, vol. 27, no. 5, pp. 368–390, 2009.

[12] G. Tavakoli Mehrjardi, F. Motarjemi, and F. Motarjemi, "Interfacial properties of geocell-reinforced granular soils," *Geotextiles and Geomembranes*, vol. 46, no. 4, pp. 384–395, 2018.

[13] T. Q. Ling, B. Zhou, C. B. Wu, and Z. N. Zheng, "Sduty of influence factors on tedons-soil interface characteristic," *Journal of Traffic and Transportation Engineering*, vol. 9, no. 5, pp. 7–12, 2009.

[14] A. M. N. Alagiyawanna, M. Sugimoto, S. Sato, and H. Toyota, "Influence of longitudinal and transverse members on geogrid pullout behavior during deformation," *Geotextiles and Geomembranes*, vol. 19, no. 8, pp. 483–507, 2001.

[15] P. Li, X. J. Huang, and Z. Liu, "Test study on the interface friction characteristics between coal gangue and gabion mesh," *Highway Engineer*, vol. 37, no. 5, pp. 83–86, 2012.

[16] C. Xu and Z. L. Shi, "Experimental research on shearing resistance property of sand-geogrid interface under cyclic load," *Rock and Soil Mechanics*, vol. 32, no. 3, pp. 655–660, 2011.

[17] I. R. Fleming, J. S. Sharma, and M. B. Jogi, "Shear strength of geomembrane–soil interface under unsaturated conditions," *Geotextiles and Geomembranes*, vol. 24, no. 5, pp. 274–284, 2006.

[18] K. M. Lee and V. R. Manjunath, "Soil-geotextile interface friction by direct shear tests," *Canadian Geotechnical Journal*, vol. 37, no. 1, pp. 238–252, 2000.

[19] Z. Duan, H. Tang, Q. Dang, F. S. Zhao, and H. Z. Lin, "Discrete element simulation of landslide induced by slop excavation," *Journal of Chang'an University (Natural Science Edition)*, vol. 34, no. 5, pp. 49–55, 2014.